AALBORG UNIVERSITY

Lithium-Ion Battery State-of-Health Estimation Using the Incremental Capacity Analysis Technique

Stroe, Daniel-Ioan; Schaltz, Erik

Lithium-Ion Battery State-of-Health Estimation Using the Incremental Capacity Analysis Technique

Daniel-Ioan Stroe
Department of Technology
Aalborg University
Aalborg, Denmark
dis@et.aau.dk

Erik Schaltz
Department of Technology
Aalborg University
Aalborg, Denmark
esc@et.aau.dk

Abstract—**The implementation of an accurate but also low computational demanding state-of-health (SOH) estimation algorithm represents a key challenge for the battery management systems in electric vehicle (EV) applications. In this paper, we investigate the suitability of the incremental capacity analysis (ICA) technique for estimating the capacity fade and subsequently the SOH of LMO/NMC-based EV Lithium-ion batteries. Based on calendar aging results collected during eleven months of testing, we were able to relate the capacity fade of the studied batteries to the evolution of four metric points, which were obtained using the ICA. Furthermore, the accuracy of the proposed models for capacity fade and SOH estimation was successfully verified considering two different aging conditions.**

Keywords—Lithium-ion Battery, SOH Estimation, Electric Vehicle, Incremental Capacity Analysis.

I. INTRODUCTION

During long time utilization, the capacity and power capability of Lithium-ion (Li-ion) batteries are subjected to gradual degradation [1]. Thus, knowledge about the batteries' state-of-health (SOH) becomes critical in practical applications (as is the case of electric vehicles - EVs), in order to ensure safe and reliable operation. Depending on the requirements of the application, the SOH can be related either to the battery capacity or to the battery internal resistance/power; for example in the case of an EV battery, the SOH is related to the capacity as the user is mainly interested in the driving range, which depends on the available battery capacity.

Different methods for Li-ion battery SOH estimation have been reported in the literature [2]. According to Berecibar et al., the SOH estimation methods can be divided into two groups [3]. The first group is using adaptive methods such as Kalman filters, neural networks or fuzzy logic to calculate the parameters of the Li-ion battery which are subjected to degradation. Most of the time, these methods are very accurate; nevertheless, they require a lot of computational power, which makes them less suitable for battery-management-system (BMS) implementation in practical applications [3]. The second group of SOH estimation methods relies on classical experimental techniques such as current pulses, coulomb counting or data maps; these methods have low computational demands and are suitable for BMS implementation, however, sometimes their accuracy is limited [3].

The SOH estimation method, which we proposed in this paper, belongs to the second group of methods and is based on the incremental capacity analysis (ICA) technique. Different authors have considered the use of the ICA technique for SOH estimation of Li-ion batteries. For example, Weng et al., have used the ICA technique in combination with support vector regression to estimate the SOH of a lithium iron phosphate (LFP)-based battery cell, which was subjected to 2300 cycles [4]. For a similar Li-ion battery chemistry, Riviere et al. in [5], built an online SOH estimator using the ICA technique. In this case, the LFP cells were aged using the NEDC driving cycle and considering a temperature of 50ºC. Even though the proposed algorithm estimates well the battery SOH, the cells using in this work are not the most suitable for EV applications. The authors in [6] investigated the use of the ICA technique for capacity estimation of an LFP-based Li-ion battery which was aged using 1800 cycles. In this work, three feature points, generated using the ICA technique, were used for battery capacity estimation; nevertheless, the model proposed for capacity estimation is using the SOC values, which is difficult to be accurately measured in real-life applications. The suitability of the ICA technique for SOH estimation of NMC-based Lithium-ion batteries is demonstrated in [7] by Li et al. Similar to the previous cases, the Li-ion batteries are aged using cycle aging conditions and no numerical model connecting the battery SOH with the features, generated using the ICA technique is provided. Berecibar et al., have proposed the ICA method for SOH estimation of NMC-based Li-ion batteries as it can detect various aging mechanism [8]. For achieving this purpose, three cells were aged at 25ºC considering three different cycle depths and; even though aging mechanism characteristic to Li-ion batteries, such as loss of lithium inventory or loss of active material, have been identified, no model for estimating the battery SOH is provided. The ICA technique was applied successfully also on Lithium-ion battery packs by Kalogiannis et al. [9]; in this work, the authors have compared and evaluated the ICA plots obtained at pack and cell level for different currents and temperatures.

Even though good SOH estimation results have been reported, in none of the abovementioned works, the ICA technique was applied to predict the SOH of Li-ion battery tailored for EV applications. Moreover, the developed SOH estimation models, if available, are difficult to be applied since they are based on other battery parameters, which are not directly measurable [6]. Consequently, for proving the suitability of the ICA technique for EV batteries' SOH estimation, we have used Li-ion batteries, specially designed for EV applications, which were subjected to twelve months of calendar aging tests carried out at different conditions.

The remainder of the paper is organized as follows. The ICA technique is introduced in Section II. The experimental set up, introducing the Li-ion battery cells use in this work and the considered aging tests are presented in Section III. The aging results and the proposed method for battery SOH estimation based on the ICA technique are introduced in Section IV, while conclusions to the work are given in Section V.

II. INCREMENTAL CAPACITY ANALYSIS TECHNIQUE

The ICA technique was initially used to study the electrochemical behavior of Li-ion batteries; more specific, ICA can be applied to analyze the lithium intercalation process and the corresponding staging phenomenon [10], [11]. Consequently, many researchers used this technique to determine the aging mechanisms, which cause the gradual capacity fade of Li-ion batteries. The ICA technique consists in differentiating the battery charging capacity against the battery voltage. In the obtained incremental capacity (IC) curve, the voltage plateaus of the charging voltage are transformed into clearly visible dQ/dV peaks (also referred to as IC peaks) [12], [13], as illustrated in Fig. 1.
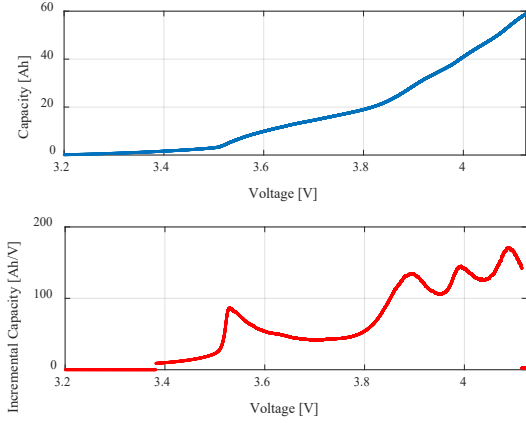

Fig. 1. Capacity (top) and IC (bottom) as a function of the battery voltage obatined for a current of 12.6 A (C/5 rate) and temperature of 25ºC.

It is worth mentioning that in order to apply the ICA technique, the charging of the battery should take place with as low as possible current since a high current strongly influences the reactions in the cells and results into distorted or undetectable IC peaks. Furthermore, in order to allow for aging analysis and SOH estimation, the capacity measurement has to be performed with a consistently current and at the same temperature, since the ICA plots are very sensitive to the changes in both these parameters (i.e., current and temperature), as shown in Fig. 2. For example, a change from C/5 to C/2 in the charging current used during the capacity measurement can results in 15 % (i.e., 18.4 Ah/V) change in the amplitude of the IC peaks. Similarly, a shift in the measurement temperature, from 15 to 30 ºC, can results in approximatively 20 % (i.e., 26.2 Ah/V) deviation in the amplitude of IC peak.
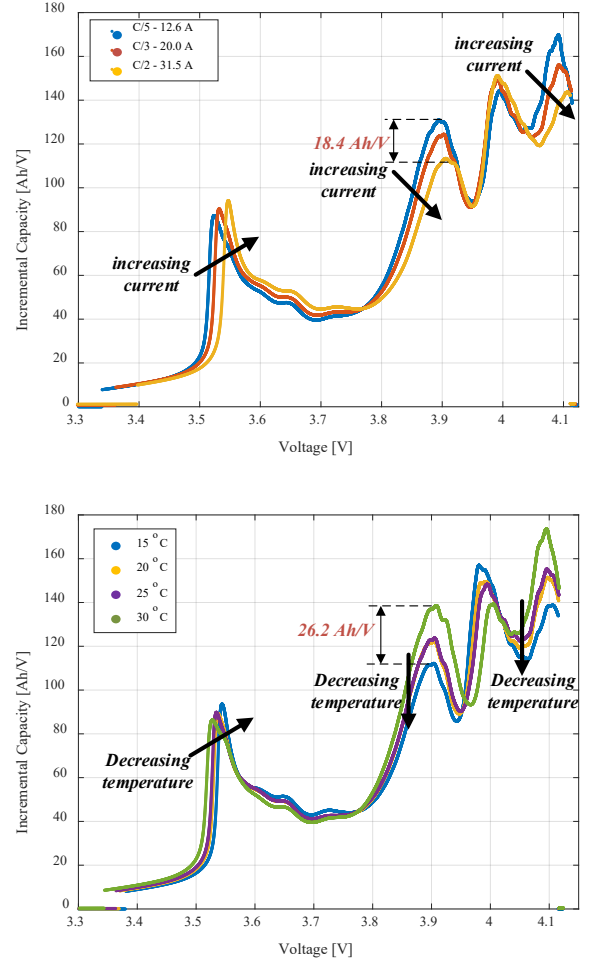

Fig. 2. Influence of the charging C-rate at 25ºC (top) and of the temperature at 12.6 A (bottom) on the IC plot; the arrows highlight the increase on the C-rate (top) and decrease in the temperature (bottom)

III. EXPERIMENT SET-UP

A. Tested Battery Cell

In this research, prismatic Li-ion battery cells with a nominal capacity of 63 Ah and a nominal voltage of 3.75 V were used (see Fig. 3). The cells are based on a graphite anode and a mixture of LMO/NMC at the cathode, Furthermore, they are specially designed for EV applications.
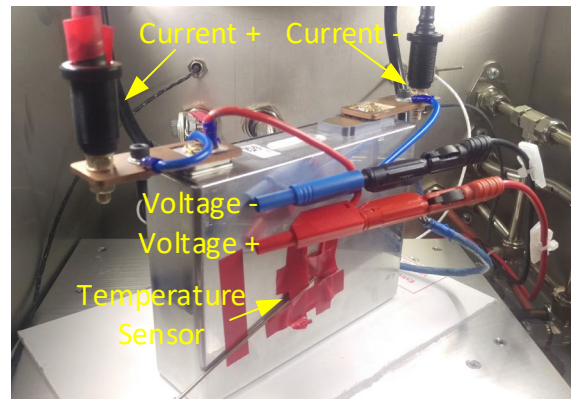

Fig. 3. LMO/NMC-based battery cell connected to the battery test station

The voltage range of the battery cell is 3 V – 4.125 V. Furthermore, at the beginning of life, the internal resistance of the cell, measured at 50% SOC and 25°C with a 1C-rate current (i.e., 63 A), is 1 mΩ.

B. Aging Conditions and Capacity Measurement

The performance (i.e., capacity and power) of Li-ion batteries are degrading during both cycle and calendar (e.g., stand-by) operation. However, there are many applications, where calendar aging represents a high percentage of battery operation during its life. For example, as it is presented in [14], batteries used in EVs spend approximately 90 to 95% of their lifetime in stand-by, during which calendar aging will occur. Furthermore, as shown by Swierczynski et al. in [15], more than 75% of the capacity fade to which a battery was subjected during EV operation was due to calendar aging. Besides EVs, another application in which batteries will degrade due to idling is uninterruptable power systems, where the batteries are scarcely used as presented in [16]. Thus, we have considered that it is relevant to investigate the degradation and to estimate the SOH of Li-ion batteries, which are aged under calendar aging conditions.

In order to consider different calendar aging scenarios, a test matrix was developed and the considered LMO/NMC-based Li-ion batteries were aged at the conditions highlighted in Table I. Each month (i.e., 30 days), the aging tests were interrupted and a reference performance test (RPT) procedure was applied to the cells. Among various parameters, the capacity of the battery cells was measured during the RPT at a temperature of 25°C. In order to comply with the requirements of the ICA technique, which demands the capacity measurement with a small C-rate, the capacity of the LMO/NMC cells was measured with C/5 (i.e., 12.6 A) during both charging and discharging. All the measurements were carried out using the Evaluator B battery test station, manufactured by FuelCon GmbH, with a voltage and current resolution of 0.1mV and 1mA, respectively. During the measurement, the data were sampled at each second.

TABLE I. CALENDAR AGING CONDITIONS FOR THE LMO/NMC BATTERY CELLS

SOC	Temperature			
	5 °C	35 °C	40 °C	45 °C
10 %				X
50 %	X	X	X	X
90 %				X

IV. RESULTS

A. Capacity Fade

The LMO/NMC-based Li-ion battery cells were aged at the calendar conditions presented in Table I for a period of 11 months. For analyzing the effect of different ageing conditions on the battery capacity, the measured capacities were normalized to the corresponding values measured at the beginning of life (BOL) according to (1). Fig. 4 and Fig. 5 present the effect on the battery capacity fade of storage temperature and storage SOC, respectively.

$$Capacity\ [\%] = Capacity_{actual} / Capacity_{BOL} \cdot 100\% \qquad (1)$$

Where $Capacity_{actual}$ [Ah] represents the battery actual capacity measured during the aging process and $Capacity_{BOL}$ [Ah] represents the battery capacity measured at the cells' BOL.
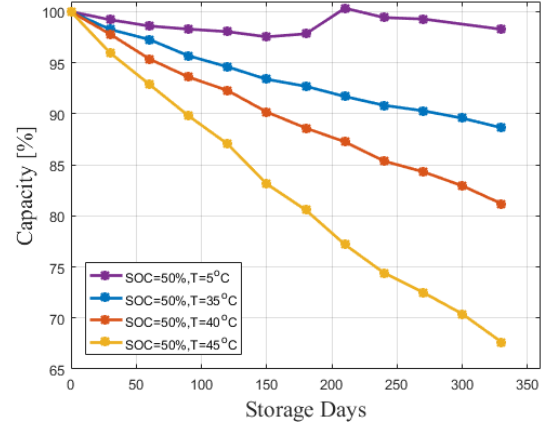

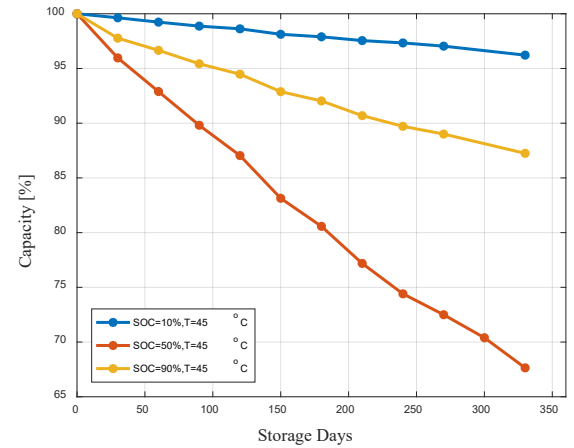Fig. 4. Capacity fade of LMO/NMC-based battery cells measured at different temperatures and SOC = 50%.

Fig. 5. Capacity fade of LMO/NMC-based battery cells measured at different SOCs and T = 45°C.

As expected, the increase of the storage temperature causes the acceleration of the capacity fade; this behavior is especially obvious for the battery cell tested at 45°C, which during the seven months of aging tests lost approximately 23% of its capacity, i.e. double than the battery cell tested at 40°C. These results are in good agreement with the behavior of NMC battery cells, which are reported for example in [17]. The influence of the storage SOC on the capacity fade of the tested LMO/NMC cells is more complex than the influence of the temperature. As it is illustrated in Fig. 4, higher capacity fade was obtained for the case when the cells were stored at a middle SOC (i.e., 50%) than for the cells stored at extreme SOCs (i.e., 10% and 90%). Similar behavior was reported by Keil and Jossen in [18] for an NCA-based Li-ion battery.

B. ICA for LMO/NMC cells

A typical ICA plot for the studied LMO/NMC-based Li-ion battery cell is presented in Fig. 6. In the figure, six zones

in the voltage interval of 3.3 V - 4.1 V are highlighted for further analysis. These six zones are defined by twelve metric points, representing four IC peaks, two IC valleys, and their corresponding six voltage values.
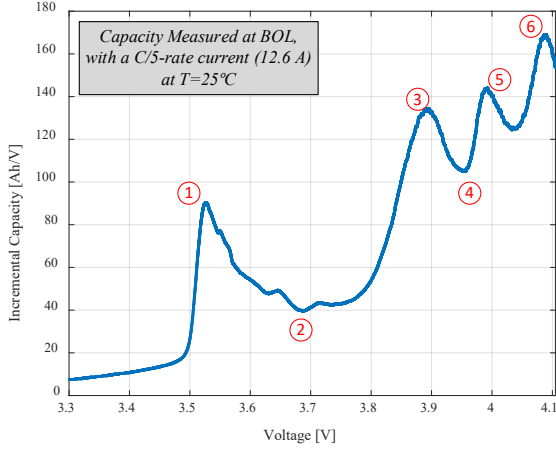

Fig. 6. ICA curve obtained for a C/5 charge of the LMO/NMC battery cells with five zones selected for further analysis.

The evolution of the ICA curves obtained during the calendar aging process for the battery cell tested at 35°C and 50% SOC is presented in Fig. 7. By analyzing these results, obtained after 11 months of aging, a-quasi monotonous displacement of the IC peaks and valleys in Zone 1, Zone 2, and Zone 4 was observed as illustrated in Fig. 8, Fig. 9, and Fig. 10, respectively. The evolutions of the IC peaks in Zone 3 and Zone 6 are scattered and no consistent aging trends were observed. Furthermore, the IC peak corresponding to Zone 5 has ceased to be visible after five months of aging. Similar behaviors were obtained for the LMO/NMC battery cells aged at the other considered conditions. Therefore, the following analysis is focused only on the results obtained for the LMO/NMC battery cell aged at 35 ºC and 50% SOC.
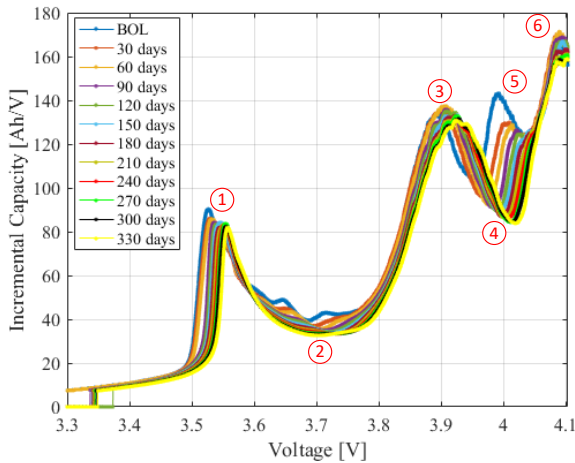

Fig. 7. Evolution of the ICA curve corresponding to the battery cell aged at T=35°C and SOC=50% (the capacity was measured at 25ºC using a current of 12.6 A (C/5 rate)).
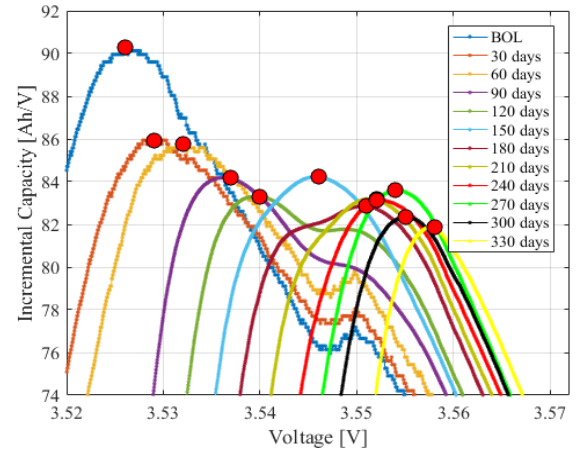

Fig. 8. Evolution of the IC peak in Zone 1 for the battery cell aged at T=35°C and SOC=50%.
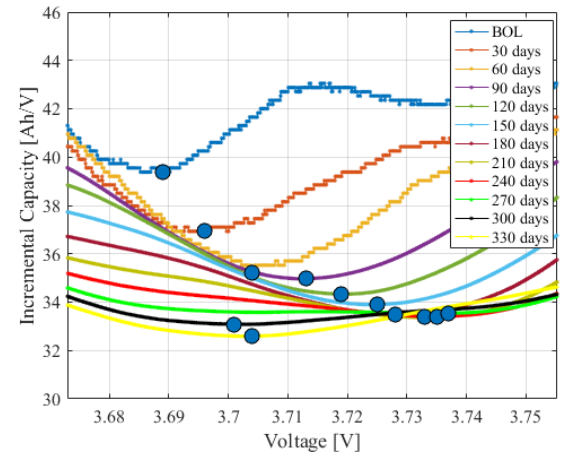

Fig. 9. Evolution of the IC valley in Zone 2 for the battery cell aged at T=35°C and SOC=50%.
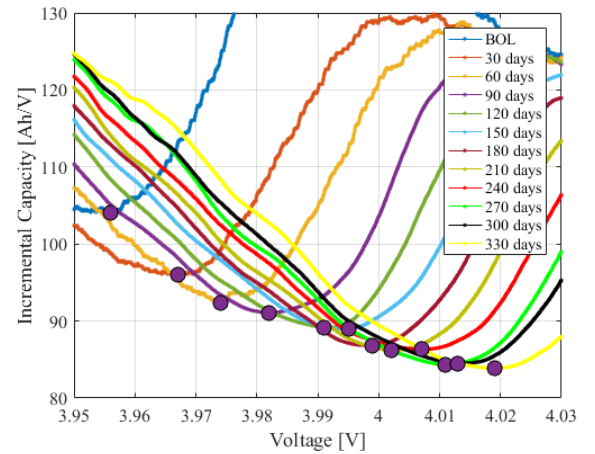

Fig. 10. Evolution of the IC valley in Zone 4 for the battery cell aged at T=35°C and SOC=50%.

C. ICA-based SOH estimation

The evolution of the peak and valleys and their corresponding voltage values, corresponding to Zone 1, Zone 2, and Zone 4 were further analyzed. Thus, based on (2), (3), and (4), we have related the values of the IC peaks and

valleys and their corresponding voltage levels, obtained during aging, to the values, which were obtained at the battery cell BOL.

$$ICpeak_{evolution} \ [\%] = ICpeak_{actual} / ICpeak_{BOL} \cdot 100\% - 100\% \quad (2)$$

$$ICvalley_{evolution} \ [\%] = ICvalley_{actual} / ICvalley_{BOL} \cdot 100\% - 100\% \quad (3)$$

$$V_{evolution} \ [\%] = V_{actual} / V_{BOL} \cdot 100\% - 100\% \quad (4)$$

Where $ICpeak_{evolution}$ represents the change in the value of the IC peak (corresponding to Zone 1) caused by aging, $ICpeak_{actual}$ represents the actual value of the IC peak measured after each month of aging, and $ICpeak_{BOL}$ represents the value of the IC peak at the battery cell's BOL. Analogical definitions are valid for $ICvalley_{evolution}$, $ICvalley_{actual}$, $ICvalley_{BOL}$, $V_{evolution}$, V_{actual}, and V_{BOL}.

The evolution of the investigated IC peak/valley value, and their corresponding voltage values, during calendar ageing, at T=35°C and SOC=50%, are presented in Fig. 11 – Fig. 16, respectively.

By analyzing the aging results presented in Fig. 11 – Fig. 16, it can be observed that the evolution of the IC peak value corresponding to Zone 1 (Fig. 11) and the evolution of the voltage value corresponding to Zone 2 (Fig. 15), are not following consistent trends. Namely, the evolution of the IC peak value corresponding to Zone 1 is not monotonous, while in the evolution of the voltage value corresponding to

Zone 2 a sudden decrease after nine months of aging takes place.

After comparing the capacity fade behavior of the LMO/NMC battery cell aged at T=35°C and SOC=50%, which is presented in Fig. 4, with the evolutions of IC metric points (e.g., peaks, valleys, voltage values), presented in Fig. 12 – Fig. 14 and Fig. 16, similar aging trends have been observed. Thus, we have plotted the battery cell capacity fade as function of the evolution of the IC metric points, which were obtained through the ICA. As presented in Fig. 17 and Fig. 18, a power-law function (5) fits with high accuracy the relationship between the battery capacity fade and the evolution of the IC valleys corresponding to Zone 2 and Zone 4, respectively. Moreover, it was found out that a linear relationship (6) exists between the evolution of the voltage value corresponding to Zone 1 and Zone 4 and the capacity fade of the LMO/NMC battery cells, as shown in Fig. 19 and Fig. 20.

$$Cfade \ [\%] = a \cdot ICvalley_{evolution}{}^{b} \quad (5)$$

$$Cfade \ [\%] = c \cdot V_{evolution} \quad (6)$$

Where C_{fade} represents the measured capacity fade of the LMO/NMC-based Li-ion battery cell, a and b represent the coefficient and exponent of the power-law fitting function, while c represents the coefficient of the linear fitting function.
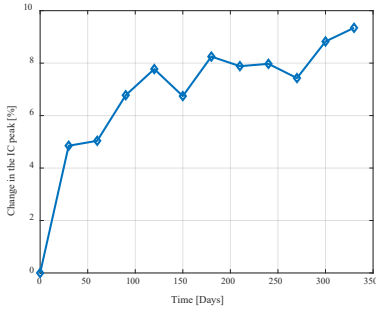

Fig. 11. Evolution during calendar aging of the IC peak value corresponding to Zone 1.
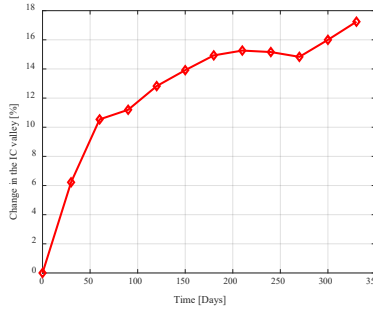

Fig. 12. Evolution during calendar aging of the IC valley value corresponding to Zone 2.
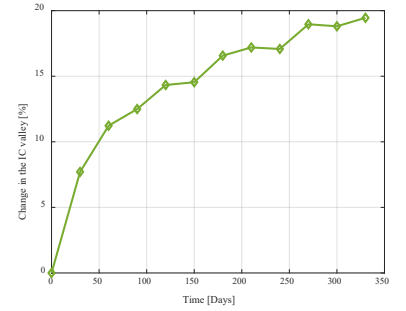

Fig. 13. Evolution during calendar aging of the IC valley value corresponding to Zone 4.
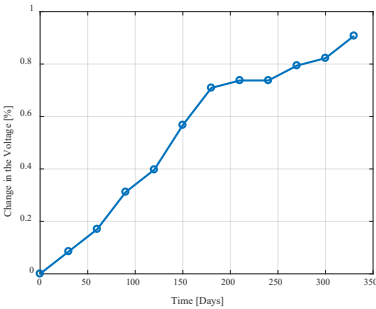

Fig. 14. Evolution during calendar aging of the voltage value corresponding to Zone 1.
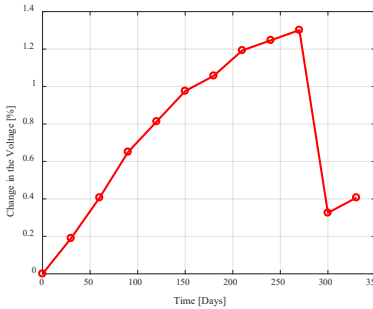

Fig. 15. Evolution during calendar aging of the voltage value corresponding to Zone 2.
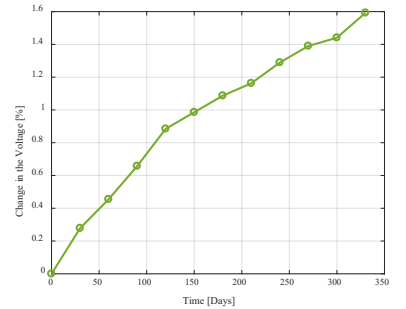

Fig. 16. Evolution during calendar aging of the voltage value corresponding to Zone 4.

Based on the results obtained from the fitting processes, it can be concluded that the capacity fade of the tested battery cells can be estimated most accurately by monitoring the evolution of the voltage value corresponding to the Zone 4, obtained by the ICA technique. In many applications (e.g., EVs, renewable energy storage), the capacity fade of the battery is directly used to express its SOH. Subsequently, based on the results presented in this section, the evolution of the voltage value corresponding to Zone 4 represents a very

accurate and promising alternative to express the SOH of the studied LMO/NMC battery cell. Thus, in order to determine the battery's SOH, the lengthy capacity measurement (carried out over the entire battery voltage interval) can be replaced by a short charge of the battery in the interval 3.95 V – 4.05 V (the zone where the targeted IC valley appears) and the application of the ICA technique.
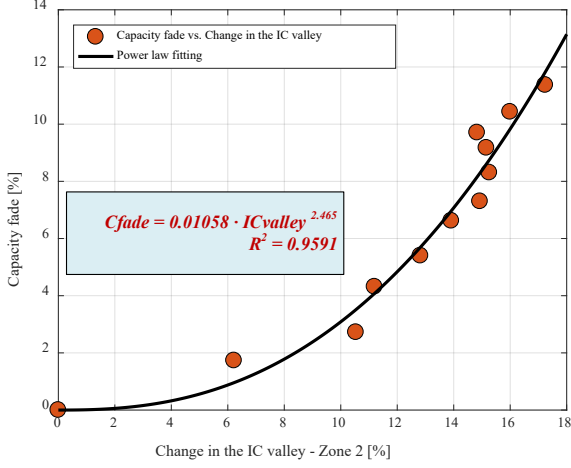

Fig. 17. Relationship between the battery capacity fade based and the IC valley evolution, corresponding to Zone 2.
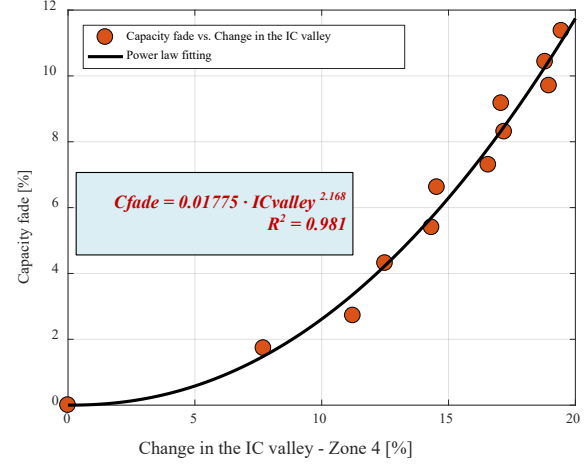

Fig. 18. Relationship between the battery capacity fade based and the IC valley evolution, corresponding to Zone 4.
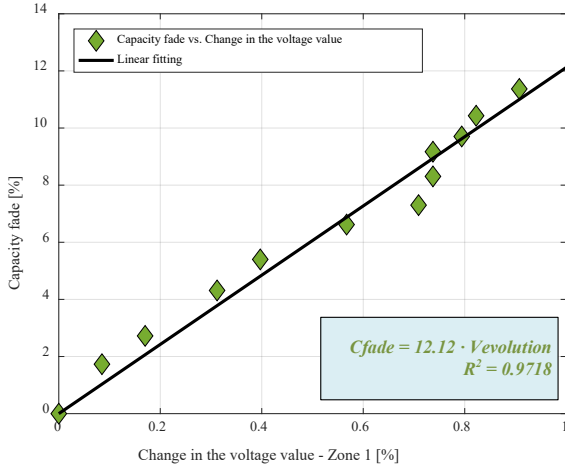

Fig. 19. Relationship between the battery capacity fade based and the voltage evolution, corresponding to Zone 1.
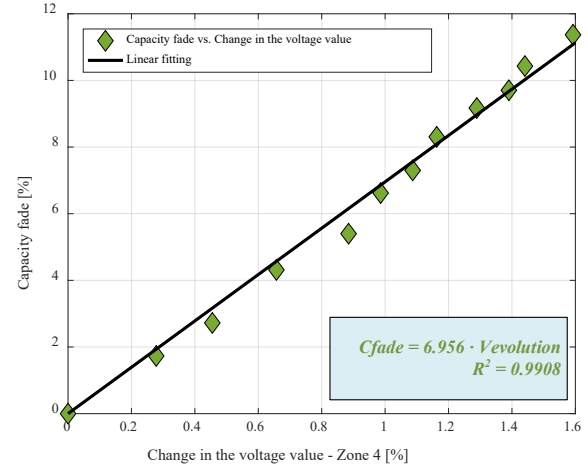

Fig. 20. Relationship between the battery capacity fade based and the voltage evolution, corresponding to Zone 4.

D. Validation

In order to validate the proposed SOH estimation models, the capacity of the considered battery was measured after 12 months of calendar aging at 35°C and 50% SOC. A discharging capacity value of 53.486 Ah, was measured, which represents a capacity fade of 12.241 %. Based on this capacity measurement, the ICA curve corresponding to 12 months of calendar aging was derived and is presented in Fig. 21.

In Fig. 21, the values of the metric points, used for SOH estimation, are highlighted. Based on these values and knowing the values at the battery cell's BOL, the SOH

estimation can be performed. The SOH obtained by applying the SOH models proposed in Fig. 17 – Fig. 20 are summarized in Table II, together with the SOH value obtained from the traditional measurements (i.e., 12.241 % capacity fade). As one can observe, the proposed models are able to estimate with high accuracy the SOH, expressed as a function of capacity, of the considered Li-ion battery. The best SOH estimation was obtained using the IC valley from Zone 4 metric point, with a 0.367% capacity fade error, and a 2.99 % normalized root-mean-square error.
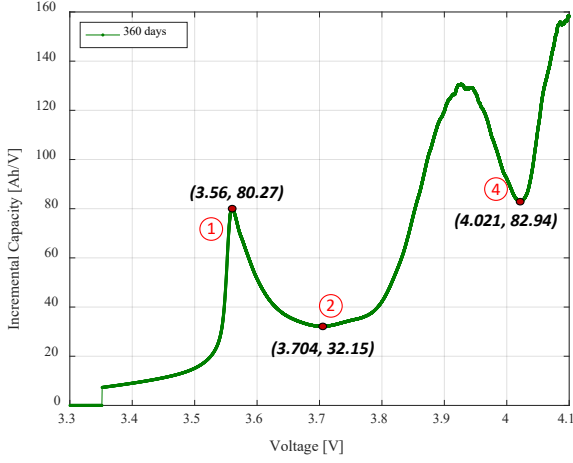
Fig. 21. ICA curve obtained after 12 months of calendar aging at 35°C and 50% SOC.

TABLE II. SOH ESTIMATION OF LMO/NMC-BASED ELECTRIC VEHICLE LITHIUM-ION BATTERY

SOH metric point	Value at BOL	Value after 12 months	Estimated SOH
IC valley – Zone 2	39.38 Ah/V	32.15 Ah/V	13.80 %
IC valley – Zone 4	104.1 Ah/V	82.94 Ah/V	11.874 %
Voltage – Zone 1	3.526 V	3.56 V	11.686 %
Voltage – Zone 4	3.956	4.021 V	11.429%
Capacity Measurement	60.947 Ah	53.486 Ah	12.241 %

Furthermore, the accuracy of the proposed SOH estimation models, which were developed for a battery cell aged at 35°C and 50% SOC, was evaluated also for the battery aged at 40°C and 50% SOC. The capacity fade behavior of the battery cell aged at 40°C and 50% SOC is presented in Fig. 4 using a red color. The evolution of the ICA curves obtained during the aging process at the aforementioned conditions is presented in Fig. 22 and the location of the SOH metric points are highlighted.
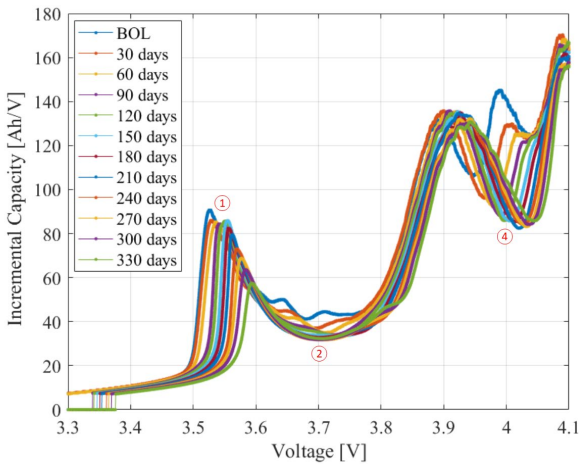

Fig. 22. Evolution of the ICA curve corresponding to the battery cell aged at T=40°C and SOC=50% (the capacity was measured at 25ºC using a current of 12.6 A (C/5 rate)).

The evolution during the eleven aging months of the values of the four considered metric points (i.e., IC valley – Zone 2, IC valley – Zone 4, Voltage – Zone 1, and Voltage – Zone 4) were applied to the developed SOH estimation models in order to estimate the battery. The obtained SOH estimation results, in terms of capacity fade, are presented in Fig. 23 and the capacity estimation errors are presented in Fig. 24 for all the four metric points. As one can observe, three out of four of the proposed SOH estimation models (i.e., except the model developed for the IC valley – Zone 2) are able to estimate accurately the capacity fade of the battery cell, for a different aging condition than the one used to parameterize the model. Moreover, it has to be highlighted that the error of the capacity fade estimation is below 3%, for the first seven months of aging. After seven months of calendar aging, a capacity fade of 12.75% was measured, which is close to the maximum capacity fade value (i.e., 12.24 %) obtained for the aging conditions for which the SOH estimation models were developed. These results might suggest that the calendar aging conditions are less important than actual capacity fade value.

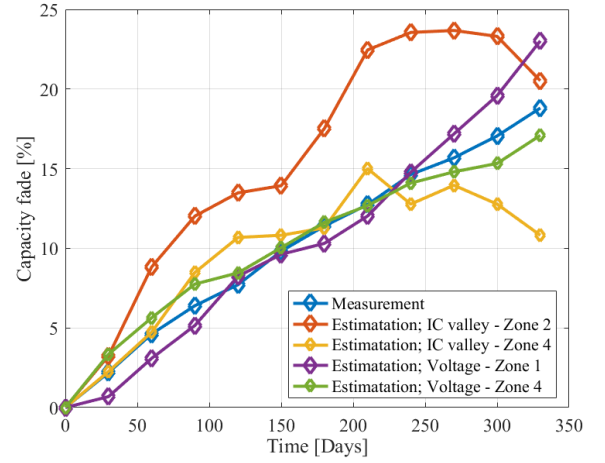Fig. 23. Capacity fade estimation using the proposed SOH estimation models; calendar aging conditions: 40°C and 50% SOC.
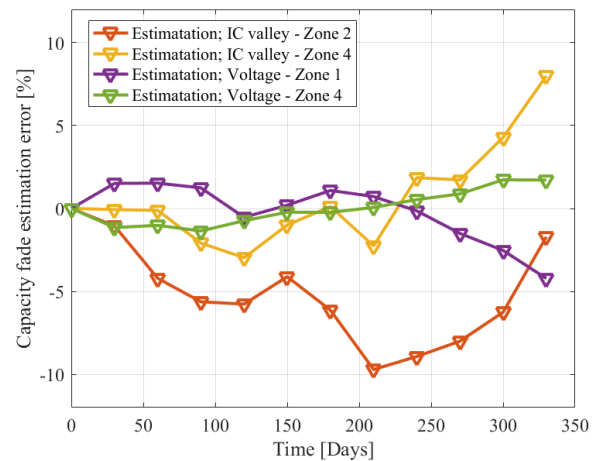

Fig. 24. Capacity fade estimation error of the proposed SOH estimation models; calendar aging conditions: 40°C and 50% SOC.

V. CONCLUSIONS

In this paper, it was shown that the ICA technique represents a reliable method for estimating the capacity fade, and subsequently the SOH of Li-ion batteries. Based on

results from eleven months of calendar aging test at 35ºC and 50% SOC, we have been able to relate the capacity fade of an LMO/NMC-based EV Li-ion battery to various peaks and valleys and their corresponding voltage values, which were obtained by applying the ICA technique.

The IC plot of the studied LMO/NMC-based battery cells is described by six different zones, which correspond to twelve metric points. Out of the twelve metric points, only four, have shown consistent aging trends during calendar aging at 35ºC and 50% SOC. By relating the evolution of these four metric points to the measured battery capacity fade, four SOH estimation models have been developed. The accuracy of these models was verified using the capacity measurement from the twelve-month of aging. Even though all the four models are estimating accurately the battery's capacity fade, the model corresponding to the IC valley from Zone 4, which corresponds to a voltage interval between 3.95V and 4.05V, has returned the best results (i.e., 0.367% capacity fade error and 2.99% normalized root-mean-square error).

Furthermore, the developed SOH estimation models were also applied to estimate the capacity fade of the battery cell, which was aged at 40ºC and 50% SOC. In this case, for three out of the four models, capacity fade estimation errors below 3% were obtained for the first seven months of calendar aging; after seven months of calendar aging, a capacity fade of 12.75% was measured, which is close to maximum capacity fade value (i.e., 12.24 %) obtained for the aging conditions (i.e., 35°C and 50% SOC) for which the SOH estimation models were developed. Nevertheless, the metric point associated with the evolution of the voltage in Zone 4 estimates very accurately (i.e., 1.7% capacity fade estimation error) the battery capacity fade for the entire calendar aging period.

Based on the results obtained from the two verification cases, it can be concluded that the metric points corresponding to Zone 4 (i.e., IC valley – first verification, voltage – second verification) are the most suitable for the SOH estimation of the tested Li-ion battery

REFERENCES

[1] D.-I. Stroe et al., "Accelerated Lifetime testing methodology for Lifetime Estimation of Lithium-Ion batteries Used in Augmented Wind Power Plants," *IEEE Transactions on Industry Applications*, vol. 50, no. 6, pp. 4006-4017, Apr. 2014.

[2] W. Waag, C. Fleischer, D.U. Sauer, "Critical review of the methods for monitoring of lithium-ion batteries in electric and hybrid vehicles," *Journal of Power Sources*, vol. 258, pp. 321-339, 2014.

[3] M. Berecibar et al., "Critical review of state of health estimation methods of Li-ion batteries for real applications," *Renewable and Sustainable Energy Reviews*, vol. 56, pp. 572-587, 2016.

[4] C. Weng, Y. Cui, J. Sun, H. Peng, "On-board state of health monitoring of lithium-ion batteries using incremental capacity analysis with support vector regression," *Journal of Power Sources*, vol. 235, pp. 36-44, 2013.

[5] E. Riviere, P. Venet, A. Sari, F, Meniere, Y. Bultel, "LiFePO4 Battery Battery State Of Health Online Estimation Using Electric Vehicle Embedeed Incremental Capacity Analysis," *Vehicle Power and Propulsion Conference (VPPC), 2015 IEEE*, pp. 1–6, 2015.

[6] L. Zheng et al., "Incremental capacity analysis and differential voltage analysis based state of charge and capacity estimation for lithium-ion batteries," *Energy*, vol. 150, pp. 759-769, 2018.

[7] Y. Li et al., "A quick on-line state of health estimation method for Li-ion battery with incremental capacity curves processed by Gaussian filter," *Journal of Power Sources*, vol. 373, pp. 40 – 53, 2018.

[8] M. Berecibar, M. Dubarry, N. Omar, I. Villareal, J. Van Mierlo, "Degradation Mechnism Detection for NMC Batteries based on incremental Capacity Curves," World Electric Vehicle Journal, vol. 8, no. 2, pp. 350-361, 2016.

[9] T. Kalogiannis, et al., "Incremental Capacity Analysis of a Lithium-Ion battery Pacl for Different Charging Rates," ECS Transactions, vol. 77, no. 11, pp. 403-412, 2017.

[10] J. Groot, "State-of-Health Estimation of Li-ion Batteries: Ageing Models," *Ph.D. Thesis*, Chalmers University of Technology, Göteborg, 2014.

[11] C. Weng, et al, "On-board state of health monitoring of lithium-ion batteries using incremental capacity analysis with support vector regression," *Journal of Power Sources*, vol. 235, pp. 36-44, 2013.

[12] M. Dubarry, V. Svoboda, R. Hwu, B. Y. Liaw, "Incremental Capacity Analysis and Close-to-Equilibrium OCV Measurements to Quantify Capacity Fade in Commercial Rechargeable Lithium Batteries," *Electrochemical and Solid-State Letters*, vol. 9, no.10, pp. A454-A457, 2006.

[13] D.-I. Stroe and E. Schaltz, "SOH Estimation of LMO/NMC-based Electric Vehicle Lithium-Ion Batteries Using the Incremental Capacity Analysis Technique," *2018 IEEE Energy Conversion Congress and Exposition (ECCE)*, Portland, OR, USA, 2018, pp. 2720-2725.

[14] A. Eddahech et al., "Remaining useful life prediction of lithium batteries in calendar ageing for automotive applications," *Microelectronics Reliability,* vol. 52, pp. 2438-2442, Sep. 2012.

[15] M. Swierczynski et al., "Suitability of the Nanophosphate LiFePO4/C Battery Chemistry for the Fully Electric Vehicle: Lifetime Perspective," *IEEE Transactions on Industry Applications*, vol. 51, no. 4, pp. 1-8, Mar. 2014.

[16] A. I. Stan et al., "A Comparative Study of Lithium Ion to Lead Acid Batteries for use in UPS Applications," in *IEEE 2014 International Telecommunications Energy Conference,* 2014, pp. 1-8.

[17] S. Käbitz et al., "Cycle and calendar life study on a graphite/ LiNi1/3Mn1/3Co1/3O2 high energy system. Part A: Full cell characterization," *Journal of Power Sources*, vol. 239, pp. 572-583, 2013.

[18] P. Keil and A. Jossen, "Calendar Aging of NCA Lithium-Ion Batteries Investigated by Differential Voltage Analysis and Coulomb Tracking," *Journal of The Electrochemical Society*, vol. 164, no. 1, pp. A6066-A6074, 2017.